Dalton Transactions

Accepted Manuscript

ROYAL SOCIETY OF CHEMISTRY

www.rsc.org/dalton

Graphical abstract:

Assembly of Co(II) salt with a new pentacarboxylic acid and five different N-donor co-ligands results in six coordination polymers. The construction of these complexes shows the N-donor co-ligands and pH value have an effect on the final structures.

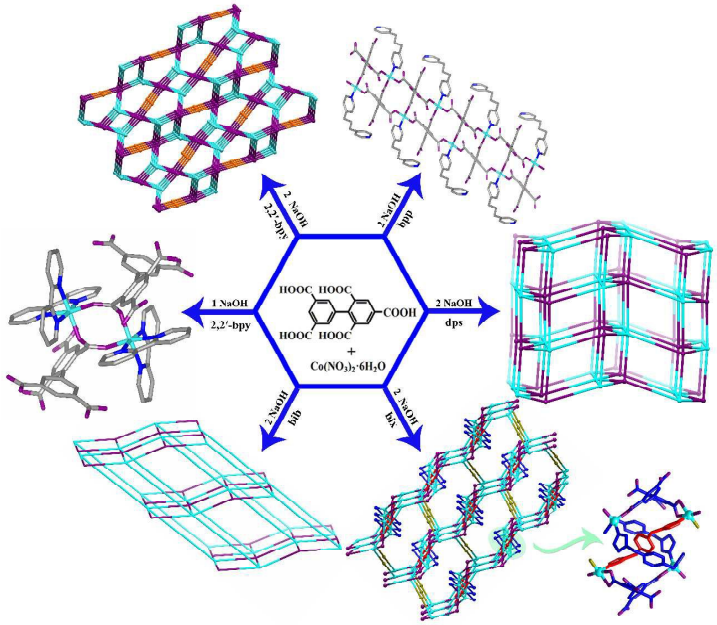

Journal Name

RSCPublishing

ARTICLE

Biphenyl-2,4,6,3',5'-pentacarboxylic acid as tecton for six new Co(II) coordination polymers: PH and N-donor ligands-dependent assemblies, structure diversities and magnetic properties

Cite this: DOI: 10.1039/x0xx00000x

Received 00th January 2012,
Accepted 00th January 2012

DOI: 10.1039/x0xx00000x

www.rsc.org/

Min-Le Han[a,b], Liang Bai[b], Ping Tang[b], Xue-Qian Wu[b], Ya-Pan Wu[b], Jun Zhao[b], Dong-Sheng Li*[,b] and Yao-Yu Wang[a]

Six new Co(II)-base mixed-ligand coordination polymers, namely, $[Co_2(H_3bppc)_2(2,2'\text{-bpy})_4]\cdot H_2O$ (**1**), $[Co_2(Hbppc)(2,2'\text{-bpy})_2(H_2O)]\cdot H_2O$ (**2**), $[Co(H_2bppc)(H\text{-bpp})]\cdot 2H_2O$ (**3**), $[Co_3(\mu_3\text{-OH})(bppc)(dps)(CH_3CH_2OH)]\cdot 4H_2O$ (**4**), $[Co_2(bppc)(bib)(H_2O)_4]\cdot(H_2\text{-bib})_{0.5}\cdot(H_2O)_3$ (**5**), $[Co_2(Hbppc)(bix)_2]\cdot 2H_2O$ (**6**), (H_5bppc = biphenyl-2,4,6,3',5'-pentacarboxylic acid, 2,2'-bpy = 2,2'-bipyridine, bpp = 1,3-bis(4- pyridyl)propane, dps = 4,4′-sulfanediyldipyridine, bib = 1,4-bis(imidazol-1-yl)benzene, bix = 1,4-bis(imidazol-1-ylmethyl)benzene), have been obtained under solvothermal conditions. **1** exhibits a 3D supramolecular framework based on $[Co_2(H_3bppc)_2(2,2'\text{-bpy})_4]$ unit. **2** has a (3,4)-connected **dmc** net with a $(4.8^2)(4.8^5)$ topology containing alternate binuclear metal clusters and single metal centres. **3** shows 3D supramolecular architecture constructed from ladder-like arrays decorated with H-bpp. **4** exhibits a binodal (5,7)-connected 3D network based on trinuclear $[Co_3(\mu_3\text{-OH})]^{5+}$ units with an unusual $(3.4^6.5^2.6)(3^2.4^6.5^7.6^5.7)$ topology. **5** features a (4,6)-connected 3D **fsc** open framework with binuclear $[Co_2(H_2O)(COO)]^{3+}$ units as nodes, and H_2-bib and water molecules located in the voids of its framework by hydrogen bonds. **6** possesses a 3D net containing unusual 2D polyrotaxane sheets. Topological analysis reveals that **6** has a (3,4,4)-connected 3D network with a $(4.6.7^4)(4.6.7)(6.7^2.10^2.11)$ topology. The structural difference of **1** and **2** is due to different pH value of reaction system. Though complexes **2**–**6** were synthesis under similar reaction conditions, the carboxylic groups of H_5bppc were partially deprotonated in **2**, **3** and **6** and fully deprotonated in **4** and **5**. Complexes **2**–**6** display diverse structures depending on different N-donor ligands and coordination modes of multicarboxylate ligand. Variable-temperature magnetic susceptibility measurements reveal that complexes **1**–**6** show antiferromagnetic interactions.

Introduction

Recently Co(II)-based coordination polymers (Co-CPs) have drawn considerable attention because of their huge diversity and versatility structure and potential applications in the areas of magnetism, catalysis, adsorption / separation, nonlinear optics etc.[1-4] A key step in the construction of such extended architectures is to employ appropriate organic bridging ligands. Among organic bridging ligands, aromatic multicarboxylate ligands such as the well-known 1,3,5-benzenetricarboxylate (BTC) and isophthalate (ip), as the mediators between the metal centres, can yield predetermined networks and have been widely employed to construct Co-CPs.[5] Some reviews have discussed the chemistry of CPs based on aromatic multicarboxylate,[6] however, the research of aromatic multicarboxylate ligands are particularly interesting due to the huge diversity and versatility of such organic blocking in the fields of crystal engineering.[7] In this context, biphenyl-2,4,6,3',5'-pentacarboxylic acid (H_5bppc) with five carboxylic groups contains all characters of two famous aromatic multicarboxylic acid ligands (H_3BTC and H_2ip, Scheme 1), which has aroused our research interest. The five carboxyl groups can induce various coordination modes and allowing higher dimensionality structures, and act as hydrogen bond acceptor/donor, depending upon the degree of deprotonation. On the other hand, two sets of carboxyl groups separated by the phenyl group can form different dihedral angles through the rotation of C–C single bonds, thus it may ligate metal centres in different orientations, which may lead to various motifs with expected function. However, only one Co-CP based on H_5bppcis reported until now.[8]

According to a survey of the previous references, the mixed ligands strategy was widely used to construct CPs. N-donor ligands have been widely utilized for tunability of structural

frameworks.[9-10] Among N-donor ligands, 2,2'-bipyridine (2,2'-bpy), a chelating ligand, often serves as terminal ligand and employed to construct CPs. Flexible and semi-flexible bis(pyridyl)/bis(imidazole) ligands can adopt different conformations with respect to the relative orientations of the linkers, which are employed to constrcut CPs with entanglement structures.[11-12] Meanwhile, flexible and semi-flexible bis(pyridyl) ligands also can serve as unidentate coordinated mode and another nitrogen atom can be protonated or not and act as hydrogen-bonding acceptor or donor.[13]

As part of our investigations on the structural diversity, magnetism and photocatalytic properties of metal aromatic polycarboxylic frameworks, some novel Co-CPswith gas adsorption and photocatalysis and magnetic properties are reported in our previous work.[14] Herein, H_5bppc was selected as a bridging ligand and reacted with Co(II) ions. Then bis(pyridyl)/bis(imidazole) ligands, 2,2'-bpy, bpp (1,3-bis(4-pyridyl)propane), dps (4,4′-sulfanediyldipyridine), bib (1,4-bis(imidazol-1-yl)benzene), and bix (1,4-bis(imidazol-1-ylmethyl)benzene) as auxiliary ligands were indroduced to reaction system, which gave rise to six Co-CPs, namely $[Co_2(H_3bppc)_2(2,2'\text{-bpy})_4]\cdot H_2O$ (**1**), $[Co_2(Hbppc)(2,2'\text{-bpy})_2(H_2O)]\cdot H_2O$ (**2**), $[Co(H_2bppc)(H\text{-bpp})]\cdot 2H_2O$ (**3**), $[Co_3(\mu_3\text{-OH})(bppc)(dps)(CH_3CH_2OH)]\cdot 4H_2O$ (**4**), $[Co_2(bppc)(bib)(H_2O)_4]\cdot(H_2\text{-bib})_{0.5}\cdot(H_2O)_3$ (**5**), $[Co_2(Hbppc)(bix)_2]\cdot 2H_2O$ (**6**). All these complexes were characterized by X-ray crystallographic, IR, elemental analysis, thermal behavior, and powder X-ray diffraction (PXRD). The magnetic properties of **1**–**6** were also investigated.

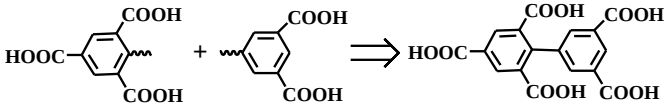

Scheme 1. Schematic representation of relation between H_3BTC and H_2ip.

Experimental

Materials and Physical Measurements

All solvents and reagents were available and were used as received. Elemental analysis for C, H, N and S was performed on a Flash2000 organic elemental analyzer. Thermogravimetric analysis was performed on a NETZSCH STA 449C microanalyzer heated from 30 to 800°C in air atmosphere. Infrared spectra (4000~600 cm^{-1}) were recorded on a NICOLET 6700 FT-IR spectrometer. Powder X-ray diffraction (PXRD) patterns were taken on a Rigaku Ultima IV diffractometer (Cu *Kα* radiation, λ = 1.5406 Å), with a scan speed of 5 °/min and a step size of 0.02° in 2θ. Variable-temperature magnetic measurements were carried out on a Quantum Design SQUID MPMS XL-7 instrument (2~300 K) in the magnetic field of 1 KOe, and the diamagnetic corrections were evaluated by using Pascal's constants.

Preparation of complexes 1-6

$[Co_2(H_3bppc)_2(2,2'\text{-bpy})_4]\cdot H_2O$ (1)

$Co(NO_3)_2\cdot 6H_2O$ (0.2 mmol, 58.2mg), H_5bppc (0.05 mmol, 18.7 mg), and 2,2'-bpy (0.2 mmol, 31.2 mg) were dissolved in EtOH-H_2O (*v*:*v* = 1:1, 10 mL), and then NaOH (0.5 mL, 0.1 M) was added. The mixture was sealed in a Teflon-lined stainless steel vessel (25 mL), and heated at 140 °C for 3 days, and then cooled to room temperature over 24 h. Violet prism crystals of **1** were obtained. Yield: 58% (based on Co(II)). Elemental analysis (%): calcd for $C_{74}H_{50}N_8O_{21}Co_2$ (M_r = 1505.08): C 59.01, H 3.35, N 7.45; found: C 58.75, H 3.32, N 7.51. IR (cm^{-1}): 3427(w), 1710(s), 1604(s), 1473(w), 1443(s), 1374(m), 1315(w), 1247(m), 1167(m), 1021(w), 773(m), 738(m).

$[Co_2(Hbppc)(2,2'\text{-bpy})_2(H_2O)]\cdot H_2O$ (2)

$Co(NO_3)_2\cdot 6H_2O$ (0.2 mmol, 58.2mg), H_5bppc (0.05 mmol, 18.7 mg), and 2,2'-bpy (0.2 mmol, 31.2 mg) were dissolved in EtOH-H_2O (*v*:*v* = 1:1, 10 mL), and then NaOH (1 mL, 0.1 M) was added. The mixture was sealed in a Teflon-lined stainless steel vessel (25 mL), and heated at140 °C for 3 days, and then cooled to room temperature over 24 h. Violet prism crystals of **2** were obtained. Yield: 62% (based on Co(II)). Elemental analysis (%): calcd for $C_{37}H_{26}N_4O_{12}Co_2$ (M_r = 836.48): C 53.13, H 3.13, N 6.70; found: C 53.19, H 3.24, N 6.58. IR (cm^{-1}): 3409 (m), 1685(w), 1605(s), 1474(w), 1442(m), 1408(w), 1356(s), 1245(m), 1188(w), 1020(w), 762(m).

$[Co(H_2bppc)(H\text{-bpp})]\cdot 2H_2O$ (3)

3 was prepared by the similar method as that described for **2**, except that bpp (0.1 mmol, 19.8 mg) instead of 2,2'-bpy. Violet prism crystals of **3** were obtained. Yield: 52% (based on Co(II)). Elemental analysis (%): calcd for $C_{27}H_{23}CoN_2O_{10}$ (M_r = 665.46): C 54.15, H 3.94, N 4.21; found: C 54.23, H 3.88, N 4.25. IR (cm^{-1}): 3442 (s), 1698(w), 1614(m), 1560(s), 1520(w), 1424(w), 1359(s), 1281(m), 1088(w), 727(m), 660(m).

$[Co_3(\mu_3\text{-OH})(bppc)(dps)(CH_3CH_2OH)]\cdot 4H_2O$ (4)

4 was prepared by the similar method as that described for **2**, except that dps (0.08 mmol, 15.0 mg) instead of 2,2'-bpy. Violet prism crystals of **4** were obtained. Yield: 46% (based on Co(II)). Elemental analysis (%): calcd for $C_{29}H_{28}N_2O_{16}SCo_3$ (M_r = 869.38): C 40.06, H 3.25, N 3.22, S 3.69; found: 40.16, H 3.12, N 3.29, S 3.78. IR (cm^{-1}): 3408(s), 1633(s), 1606(w), 1589(s), 1482(w), 1431(w), 1359(s), 1281(m), 1107(w), 818(m), 767(m), 721(s).

$[Co_2(bppc)(bib)(H_2O)_4]\cdot(H_2\text{-bib})_{0.5}\cdot(H_2O)_3$ (5)

5 was prepared by the similar method as that described for **2**, except that bib (0.1mmol, 21.0 mg) instead of 2,2'-bpy. Red block crystals of **5** were obtained. Yield: 65% (based on Co(II)). Elemental analysis (%): calcd for $C_{35}H_{35}N_6O_{17}Co_2$ (M_r = 929.55): C 45.22, H 3.80, N 9.04; found: C 45.36, H 3.69, N 9.12. IR (cm^{-1}): 3383(w), 1609(w), 1538(s), 1473(w), 1429(m), 1365(s), 1311(m), 1060(w), 818(m), 960(m), 837(m), 748(w), 709(m).

$[Co_2(Hbppc)(bix)_2]\cdot 2H_2O$ (6)

6 was prepared by the similar method as that described for **2**, except that bix (0.1mmol, 23.8 mg) instead of 2,2'-bpy. Violet prism crystals of **6** were obtained. Yield: 59% (based on Co(II)). Elemental analysis (%): calcd for $C_{45}H_{35}N_8O_{11}Co_2$ (M_r = 981.67): C 55.06, H 3.59, N 11.41; found: C 55.15, H 3.51, N 11.52. IR (cm^{-1}): 3442(s), 1698(w), 1614 (m), 1559(s), 1520(w), 1423(w), 1359(s), 1281(m), 1088(w), 727(m).

X-ray Crystallography

Single crystal X-ray diffraction data for complexes **1**–**6** were collected on a Rigaku XtaLAB mini diffractometer equipped with a graphite monochromated Mo *Kα* radiation (λ = 0.71073 Å) by using φ/ω scan technique at room temperature. All structures were solved by direct methods and all non-hydrogen atoms were refined anisotropically by the full-matrix least-squares method with the SHELXTL crystallographic software package. H atoms were assigned with isotropic displacement factors and included in the final refinement with geometrical restrains. In complex **4**, ethanol molecules are disordered. There are large solvent accessible void volumes in the crystal of

Table 1. Crystal and Structure Refinement Data for Complexes **1**–**6**.

Complex	1	2	3	4	5	6
Formula	$C_{74}H_{50}N_8O_{21}Co_2$	$C_{37}H_{26}N_4O_{12}Co_2$	$C_{30}H_{26}N_2O_{12}Co$	$C_{29}H_{28}N_2O_{16}SCo_3$	$C_{35}H_{35}N_6O_{17}Co_2$	$C_{45}H_{38}N_8O_{12}Co_2$
Formula weight	1505.08	836.48	665.46	869.38	929.55	1000.69
Temperature/K	296(2)	296(2)	296(2)	296(2)	296(2)	296(2)
Crystal system	Monoclinic	Monoclinic	Monoclinic	Monoclinic	Triclinic	Monoclinic
Space group	$P2_1/c$	$P2_1/n$	$P2_1/c$	$P2_1/n$	P-1	$P2_1/n$
a/Å	12.539(7)	12.610(7)	8.887(5)	11.835(4)	10.553(4)	19.267(7)
b/Å	15.879(9)	15.935(9)	13.014(6)	19.624(6)	12.789(6)	12.221(4)
c/Å	19.394(9)	17.477(10)	25.860(14)	14.327(4)	14.443(6)	24.163(7)
α/°	90	90	90	90	112.206(6)	90
β/°	120.25(3)	101.498(8)	99.819(5)	90.519(3)	90.401(5)	125.38(2)
γ/°	90	90	90	90	94.839(2)	90
V/Å^3	3336(3)	3441(3)	2947(3)	3327.2(17)	1796.7(13)	4639(3)
Z	2	4	4	4	2	4
D_c/g·cm^{-3}	1.498	1.614	1.500	1.736	1.718	1.381
μ/mm^{-1}	0.582	1.038	0.652	1.600	1.000	0.780
F(000)	1524	1664	1372	1604	894	1976
Reflns. collected	29790	29445	23939	29724	16406	41142
Independent data	6212	6167	5318	6199	6665	8631
R_{int}	0.0730	0.0960	0.0995	0.0910	0.0400	0.1401
GOOF	1.136	1.078	1.059	1.092	1.037	1.076
R_1[a]	0.0603	0.0810	0.0648	0.0411	0.0516	0.0590
wR_2[b] [$I>2\sigma(I)$]	0.1543	0.2013	0.1752	0.1173	0.1416	0.1541
R_1 (all data)	0.0702	0.1078	0.0713	0.0432	0.0579	0.0665
wR_2 (all data)	0.1617	0.2250	0.1821	0.1190	0.1465	0.1626

[a] $R_1 = \Sigma(||F_o| - |F_c||)/\Sigma|F_o|$; [b] $wR_2 = \{\Sigma[w(|F_o|^2 - |F_c|^2)^2]/\Sigma[w(|F_o|^2)^2]\}^{1/2}$.

1, **2**, **4**–**6** which are occupied by highly disordered free water molecules. No satisfactory disorder model could be achieved, therefore the SQUEEZE program implemented in PLATON was used to remove these electron densities.[15] The crystallographic data and selected bond lengths and angles for complexes **1**–**6** are listed in Tables 1 and S2, Electronic Supplementary Information, respectively. CCDC reference No: 1061721-1061726 for complexes **1**–**6**, respectively.

Results and Discussion

Description of Crystal Structures

$[Co_2(H_3bppc)_2(2,2'\text{-bpy})_4]\cdot H_2O$ (1). As shown in Fig.1a, Co1 centre takes a distorted octahedron geometry with two oxygen atoms (O1 and O2#1) from two H_3bppc^{2-} ligands and four three carboxylic oxygen atoms (O3, O6#1, O11#2) from three $bppc^{5-}$ ligands and one oxygen atom (O1) from μ_3-hydroxyl group. Co2 adopts a distorted trigonal-bipyramidal coordination environment, in which three carboxylic oxygen atoms (O2, O5#3, and O8#4) from three $bppc^{5-}$ ligands form the equatorial plane and the apical positions are occupied by O1 and N1 from nitrogen atoms (N1, N2, N3 and N4) from two 2,2'-bpy. In **1**, 2,3'-carboxylic groups of H_3bppc^{2-} are deprotonated and only 2-carboxylate displays (κ^1,κ^1)-μ_2 coordination fashion to link two Co(II) atoms (Scheme 2a). The adjacent Co(II) atoms are linked by two μ_2-carboxylate groups in *syn-syn* fashion to form a $[Co_2(H_3bppc)_2(2,2'\text{-bpy})_4]$ unit with a Co···Co distance of 4.69 Å (Fig. 1b). Such units are further connected by hydrogen bonding among H_3bppc^{2-} ligands and free water molecules (d(O···O) = 2.56, 2.65, and 2.82 Å) to generate a 3D supramolecular architecture (Fig. 1c, Table S2, ESI).

$[Co_2(Hbppc)(2,2'\text{-bpy})_2(H_2O)]\cdot H_2O$ (2). The asymmetric unit of **2** has two crystallographically independent Co(II) centres, one $Hbppc^{4-}$ ligand, two 2,2'-bpy, one coordinated water and one free water molecule. As shown in Fig. 2a, Co1 takes a distorted octahedron geometry with two oxygen atoms (O1 and O2#1) from two $Hbppc^{4-}$ ligands and four nitrogen atoms (N1, N2, N3 and N4) from two 2,2'-bpy, similar that in **1**. The Co2 centre owns a distorted tetrahedral geometry, coordinated by three O atoms (O5#3, O7, O10#2) from three $Hbppc^{4-}$ ligands and one coordinated water. In **2**, 4-carboxylic group of $Hbppc^{4-}$ is protonated and free of coordination. The other four carboxylate groups of $Hbppc^{4-}$ ligand adopt the $(\kappa^1\text{-}\kappa^1)$-$(\kappa^1)$-$(\kappa^1)$-$\mu_5$ coordination fashion to bridge two Co1 and three Co2 (Scheme 2b). Two adjacent Co1 are joined by two carboxylate groups of two $Hbppc^{4-}$ ligands in *syn-anti* fashion to form a binuclear $[Co_2(COO)_2(2,2'\text{-bpy})_4]^{2+}$ unit with a Co···Co distance of 4.68 Å. Co2 atoms are linked by $Hbppc^{4-}$ ligands to generate a 2D network (see Fig. 2b). The 2D layers are further joined through binuclear $[Co_2(COO)_2(2,2'\text{-bpy})_4]$ unit (Fig. 2c) to form a 3D net.

With further topological analysis, the binuclear $[Co_2(COO)_2(2,2'\text{-bpy})_4]^{2+}$ unit can be simplified as 2-connected node as a spacer, while Co2 and $Hbppc^{4-}$ can be considered as 3-connected and 4-connected nodes, respectively. Thus, the 3D structure of **2** can be described as an unusual (3,4)-connected **dmc** net with a $(4.8^2)(4.8^5)$ topology (Fig. 2d).

$[Co(H_2bppc)(H\text{-bpp})]\cdot 2H_2O$ (3). The asymmetric unit of **3** contains one Co(II) atom, one H_2bppc^{3-} ligand, one H-bpp, and two free water molecules. The Co1 centre is four coordinated and resides in a distorted tetrahedral environment with three O atoms (O1, O6#1, and O7#2) from three H_2bppc^{3-} ligands and one nitrogen atom (N1) from an unidentate H-bpp (Fig.3a). In **3**, 3',4-carboxylic groups of H_2bppc^{3-} are protonated and free of coordination. H_2bppc^{3-} ligand adopts the (κ^1)-(κ^1)-(κ^1)-μ_3 coordination fashion to link three Co1 atoms (Scheme 2c). The H-bpp ligand adopts an unidentate coordinated mode and the N2 atom is protonated and acts as the hydrogen-bonding donor. The adjacent Co(II) atoms are linked by μ_3-H_2bppc^{3-} ligands, giving rise to a ladder-like array decorated with H-bpp ligands at two sides in an outward fashion, running along the *a*-direction (Fig. 3b). The 1D arrays are linked by hydrogen bonds O···O and N···O (d(O···O) = 2.67Å, and d(N···O) = 2.76 Å) to afford a 3D supramolecular architecture (Fig. 3c, Table S2, ESI).

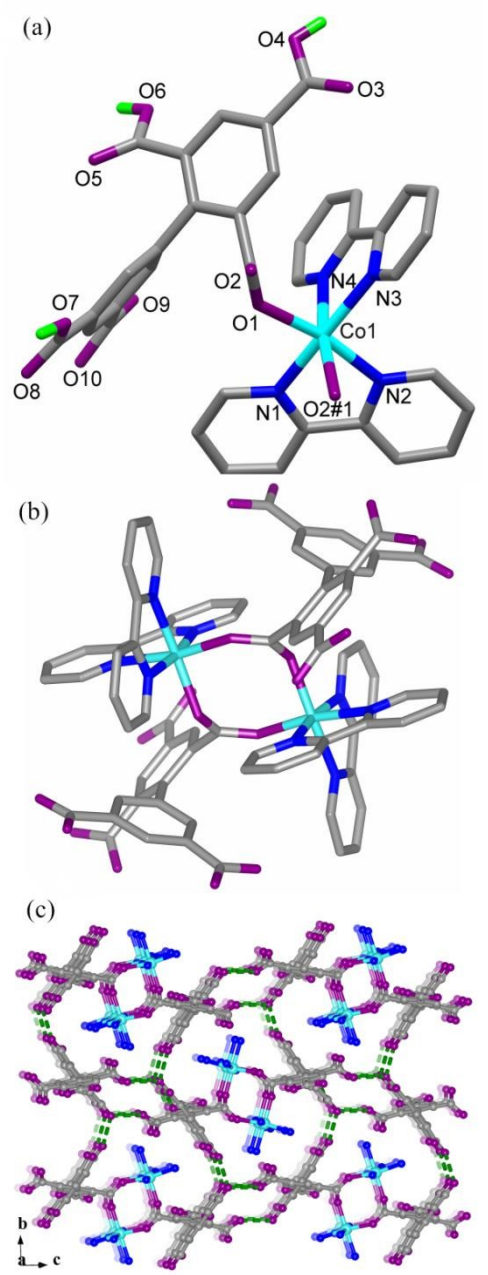

Fig. 1 (a) Coordination environment of Co(II) ion in **1** (symmetry codes: #1, -x,-y+1,-z). (b) View of the binuclear unit. (c) View of 3D supramolecular structure. Hydrogen bonds are represented as light orange dash line. C atoms of 2,2′-bpy are omitted for clarity.

$[Co_3(\mu_3\text{-}OH)(bppc)(dps)(CH_3CH_2OH)]\cdot 4H_2O$ (4). Complex **4** has a (5,7)-connected3D net with the trinuclear $[Co_3(\mu_3\text{-}OH)]^{5+}$ clusters. As illustrated in Fig. 4a, there are three crystallographic independent Co(II) ions: Co1 adopts a distorted tetrahedral coordination environment coordinated by μ_3-hydroxyl group and dps ligand with O1-Co2-N1 angle of 155.11 º. Co3 is six coordinated and resides in a distorted octahedral coordination geometry with three carboxylic oxygen atoms (O10#2, O4#3, O9#4) from three $bppc^{5-}$ ligands, one oxygen atom (O1) from μ_3-hydroxyl group, one oxygen atom (O12) from CH_3CH_2OH, and one nitrogen atom of dps. The distances of Co···Co bridged by the μ_3-hydroxyl group are 3.34, 3.40, and 3.52Å, respectively. $Bppc^{5-}$ ligand displays $(\kappa^1\text{-}\kappa^1)\text{-}(\kappa^1\text{-}\kappa^1)\text{-}(\kappa^1)\text{-}(\kappa^1\text{-}\kappa^1)\text{-}(\kappa^1\text{-}\kappa^1)\text{-}\mu_9$ binding fashion to link three Co1 atoms, three Co2 atoms and three Co3 atoms (Scheme 2d). The trinuclear units are linked through $bppc^{5-}$ ligands and dps ligands to generate a 3D framework (Fig. 4b).

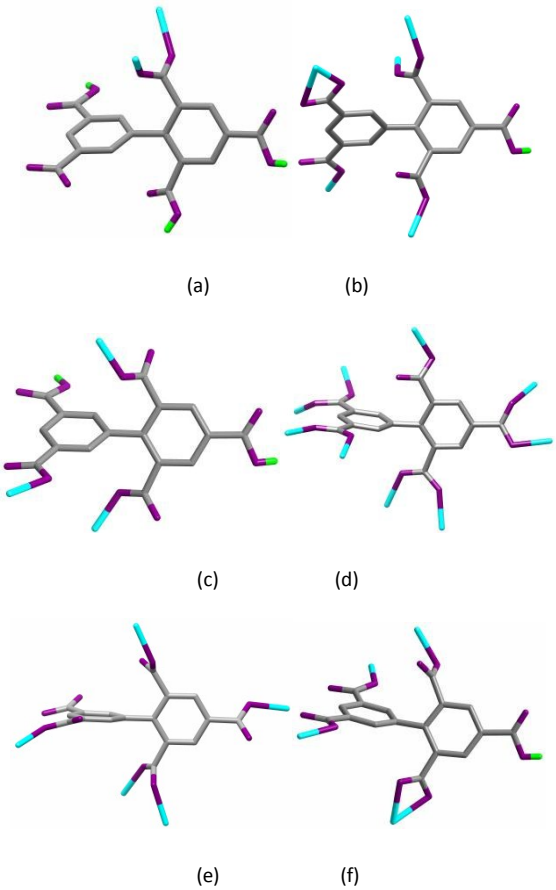

Scheme 2. Coordination modes of multicarboxylic acid ligand in this work (a for **1**, b for **2**, c for **3**, d for **4**, e for **5** and f for **6**).

Analysis of the network topology of **4** reveals that each trinuclear $[Co_3(\mu_3\text{-}OH)]^{5+}$ unit acts as a 7-connected node to connect five $bppc^{5-}$ and two trinuclear units *via* two dps spacers. $Bppc^{5-}$ serves as 5-connected node to connect five trinuclear $[Co_3(\mu_3\text{-}OH)]^{5+}$ units. Thus, an unprecedented (5,7)-connected binodal net with the point symbol of $(3.4^6.5^2.6)(3^2.4^6.5^7.6^5.7)$ is formed (Fig.4c).

Only two interesting binodal (5,7)-connected 3D CPs have been reported in the literatures.[16] $[Co_2(DCP)(1,3\text{-}bib)]_n$ displays a 3D (5,7)-connected net based on binuclear $\{Co_2\}$ units with the point symbol $(3.4^4.5^4.6)(3^2.4^8.5^8.6^3)$.[16a] $Cd_2(SA)(obix)$ features a (5,7)-connected **she** net.[16b]

$[Co_2(bppc)(bib)(H_2O)_4]\cdot(H_2\text{-}bib)_{0.5}\cdot(H_2O)_3$ (5). There are two crystallographic independent Co(II) atoms with similar distorted octahedral coordination sphere, one $bppc^{5-}$ligand, one bib ligand, four coordination water molecules, as well as half of free bib and three water molecules (Fig. 5a). Co1 is six-coordinated by three oxygen atoms (O1, O5#2, and O10#1) from three $bppc^{5-}$ ligands, two coordinated water molecules (O11 and O12) and one nitrogen atom (N1) from bib. The Co2 centre is coordinated by two carboxylic oxygen atoms (O7#4

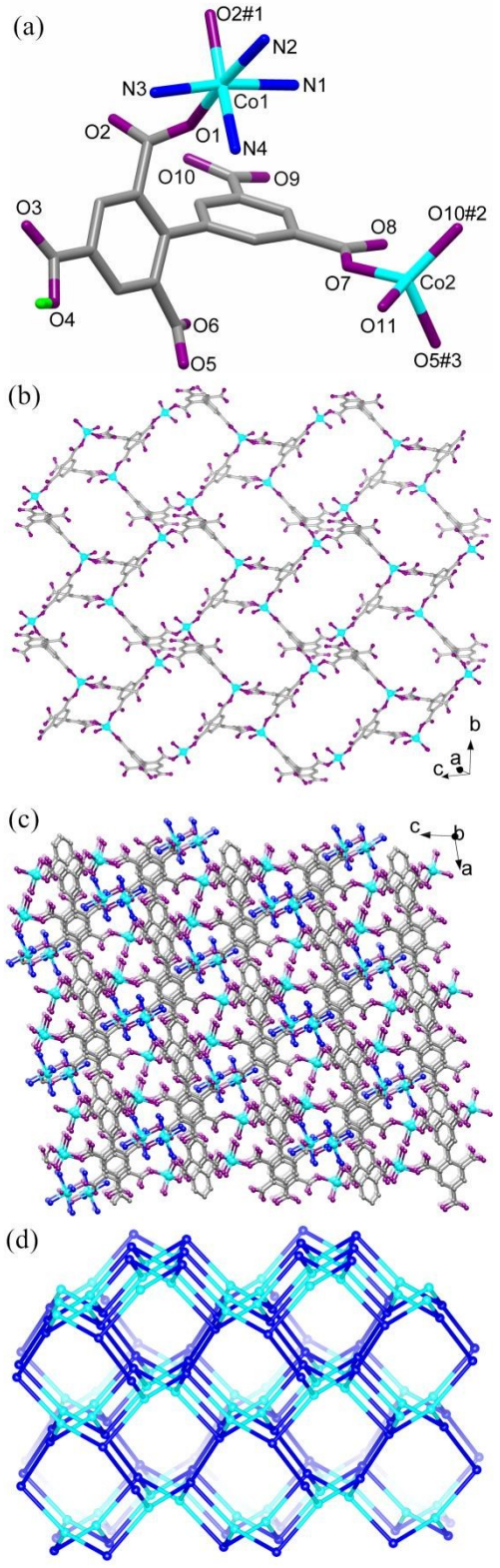

Fig. 2 (a) Coordination environments of Co(II) in **2** (symmetry codes: #1, -x+1,-y+1,-z; #2, -x+1/2,y-1/2,-z+1/2; #3, -x+1,-y+1,-z+1/2). (b) View of the 2D layer constructed by Co2 and $Hbppc^{4-}$ ligand. (c) View of 3D net. C atoms of 2,2′-bpy are omitted for clarity. (d) Schematic representation of the (3,4)-connected **dmc** net of **2**.

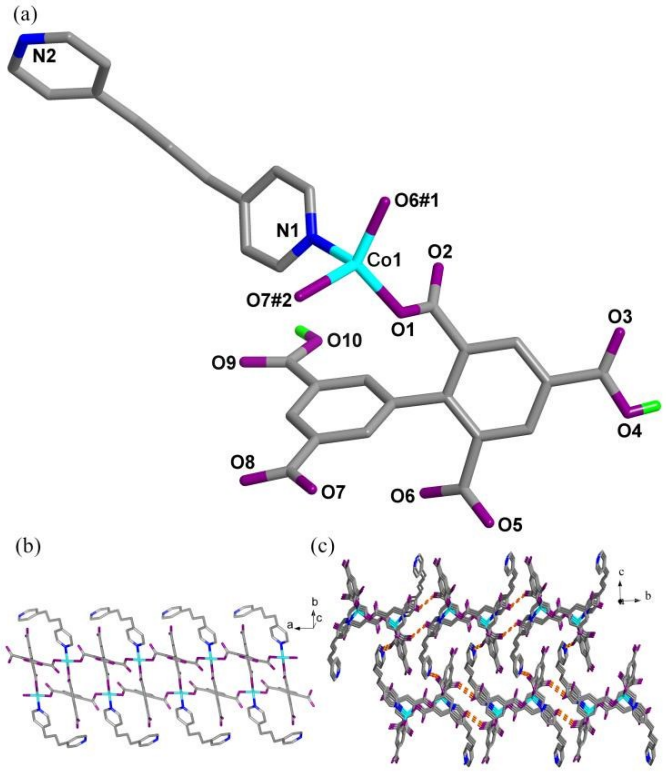

Fig. 3 (a) Coordination environment of Co(II) ion in **3** (symmetry codes: #1, x-1,y,z; #2, -x+1,-y,-z). (b) View of the 1D chain of **3**. (c) View of 3D supramolecular structure. Hydrogen bonds are represented as light orange dash line.

and O9) from two $bppc^{5-}$ ligands, three coordinated water (O12#1, O13, and O14) and one nitrogen atom (N4#3) from two bib. Co1 and Co2#1 are linked by μ_2-H_2O and one carboxylic group in *syn-syn* fashion to form a binuclear $[Co_2(H_2O)(COO)]^{3+}$ unit with the Co···Co distance of 3.80 Å. The $bppc^{5-}$ ligand adopts the $(\kappa^1\text{-}\kappa^1)\text{-}(\kappa^1)\text{-}(\kappa^1)\text{-}(\kappa^1)\text{-}\mu_5$ coordination fashion to connect three Co1 and two Co2 (Scheme 2e). The binuclear $[Co_2(H_2O)(COO)]^{3+}$ units are bridged by $bppc^{5-}$ ligands to form a 2D sheet (Fig. 5b). Such 2D sheets are further interlinked by bib ligands to form a 3D open network. The free H_2-bib and water molecules filled in the voids of the 3D net (see Fig. 5c). Without guest molecules, the effective free volume of **5**, calculated by PLATON,[16] is 20.9% of the crystal volume (375.4 $Å^3$ of the 1796.7 $Å^3$ unit cell volume).

Analysis of the network topology of **5** reveals that the binuclear cluster acts as a 6-connected node to connect four $bppc^{5-}$ and two binuclear units *via* two bib spacers. And the $bppc^{5-}$ ligand serves as a 4-connected node to connect four binuclear units. Thus, the 3D structure of **5** can be described as a binodal (4,6)-connected **fsc**-$(5^2.6^2.7.9)(5^2.6^4.7^3.8)_2(5^2.6)_2(6^3.7^2.9)$ net.

$[Co_2(Hbppc)(bix)_2]\cdot 2H_2O$ (6). The crystal structure of **6** shows a 3D network containing 2D polyrotaxane sheet. As depicted in Fig.6a, there are two crystallographic independent Co(II) ions, one $Hbppc^{4-}$, one and two half of bix ligands as well as two free water molecules. Co1 takes a distorted trigonal-bipyramidal coordination environment finished by three O atoms (O1, O2 and O7#1) from two $Hbppc^{4-}$ ligands and two N atoms (N5 and N7) from two bix. Co2 ions are four-coordinated by two O (O6 and O10#2) from two $Hbppc^{4-}$ ligands and two N atoms (N1

Journal Name RSCPublishing

ARTICLE

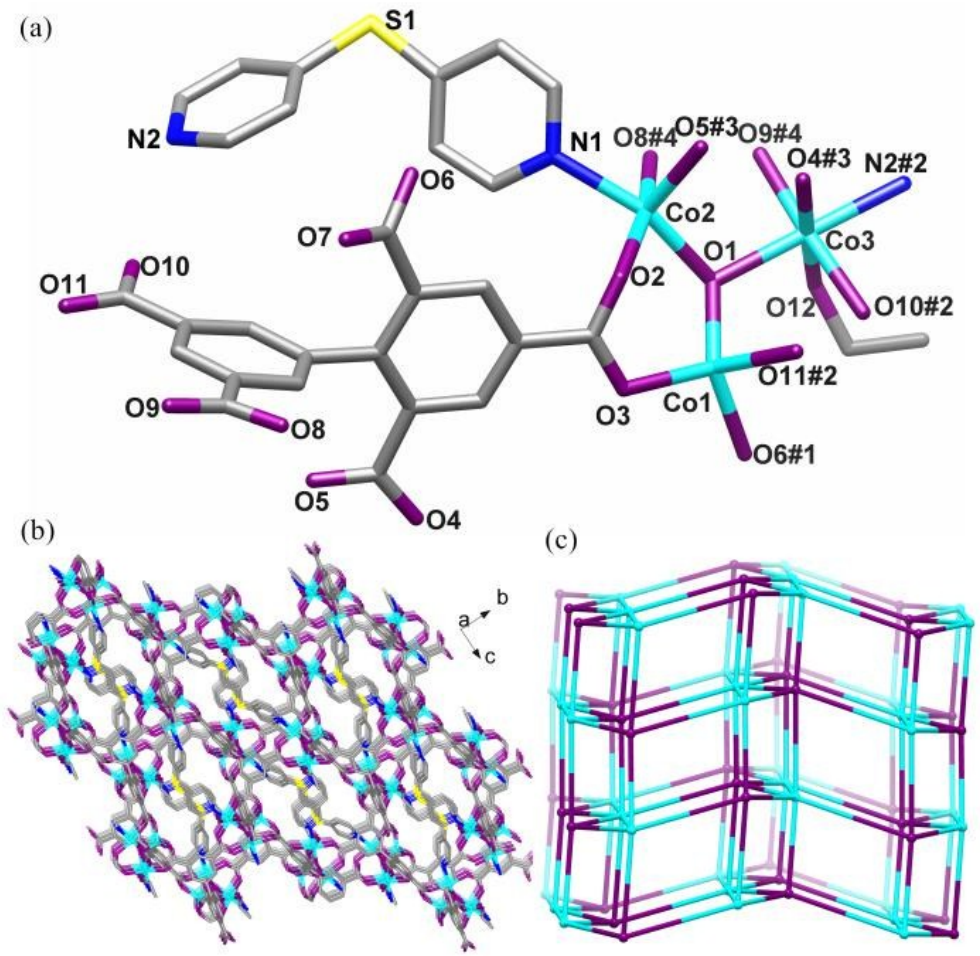

Fig. 4 (a) Coordination environments of Co(II) ion in **4** (symmetry codes: #1, x-1/2,-y+1/2,z+1/2; #2, x,y,z+1; #3, x+1/2,-y+1/2,z+1/2; #4, -x+1/2,y-1/2,-z+1/2). (b) View of 3D net. (c) Schematic representation of the binodal (5,7)-connected network.

and N4) from two bix. In **6**, 4-carboxylic group of $Hbppc^{4-}$ is protonated and free of coordination. Other carboxylate groups of $Hbppc^{4-}$ ligand link four Co(II) in the $(\kappa^1\text{-}\kappa^1)\text{-}(\kappa^1)\text{-}(\kappa^1)\text{-}(\kappa^1)\text{-}\mu_4$ coordination fashion (Scheme 2f). There are three independent bix ligands (Scheme 3), which adopt end-imidazole nitrogen atoms to link Co atoms with the Co···Co separations being 10.25 (*cix*-bix), 13.16 (*trans*-bix-A) and 15.22 Å (*trans*-bix-B), respectively. Co(II) atoms are connected by $Hbppc^{4-}$ ligand to form a 2D layer (Fig. S1, SI), in which adjacent Co2 atoms are bridged by two *cis*-bix ligands in double-bridging fashion to form a 26-membered ring $\{Co2_2(cix\text{-bix})_2\}$, creating a 'loop'. It is interesting that the $\{Co2_2(cix\text{-bix})_2\}$ 'loops' encapsulate *trans*-bix-A *via* Co2-N5, resulting in a unique 2D polyrotaxane layer (Figs. 6b and 6c). The *trans*-bix-B connect with two different 2D polyrotaxane layers, giving rise to a 3D net (see Fig. 6d and 6e).

From the view of topology, Co2 serve as 3-connect nodes, while Co1 and $Hbppc^{4-}$ ligand serve as 4-connected nodes. As a result, a trinodal (3,4,4)-connected 3D network with the point symbol of $(4.6.7^4)(4.6.7)(6.7^2.10^2.11)$ is formed (Fig. S2). Reduction of the whole structure to a (3,4,4)-connected 3D network converts the $\{Co2_2(cix\text{-bix})_2\}$ 'loop' into a single link, resulting in a network description which cannot properly describe the topology of polyrotaxane as it would require links to pass through the middle of other links. Thus to obtain a network description that can be used to further describe the polyrotaxane, one must include the 2-membered rings (*i.e.* the 'loops'), resulting in a 4-connected $(4.2.7^2.6^2)_2(4^7.4.6)_2(7.6.7.10^2.11)_2$ topology (Fig. 6e).[17]

Three interesting 3D non-interpenetrated polyrotaxane MOFs have been reported.[18] $\{[Cd_3(nbta)_2(bpy)_5(H_2O)_2]\cdot 6H_2O\}_n$ features a polyrotaxane (3,5,6)-connected 3D network with a $(5^2.6^4.7^2.8^6.10)(5^2.6^5.7^2.8)(5^2.6)_2$ topology.[18a] In $\{[Cd_2(TPPA)_2(DCPS)_2]\}_n\cdot x$solvent, the 1D Cd-DCPS straps

can be simplified into two connected successions of loops. Each two loops on the two layers are connected by Cd-O bonds and further thread by two arms of two TPPA ligands from the two sides, which represents the rotaxane unit. The other two arms of each TPPA ligand connect with two different 1D straps, which gives rise to a 3D polyrotaxane net.[18b] $[Cd(bpeb)_{0.5}(poly\text{-}bppcb)_{0.5}(sdb)]\cdot DMA$ displays a (3,4)-connected 3D polyrotaxane net with a **tfc** topology.[18c]

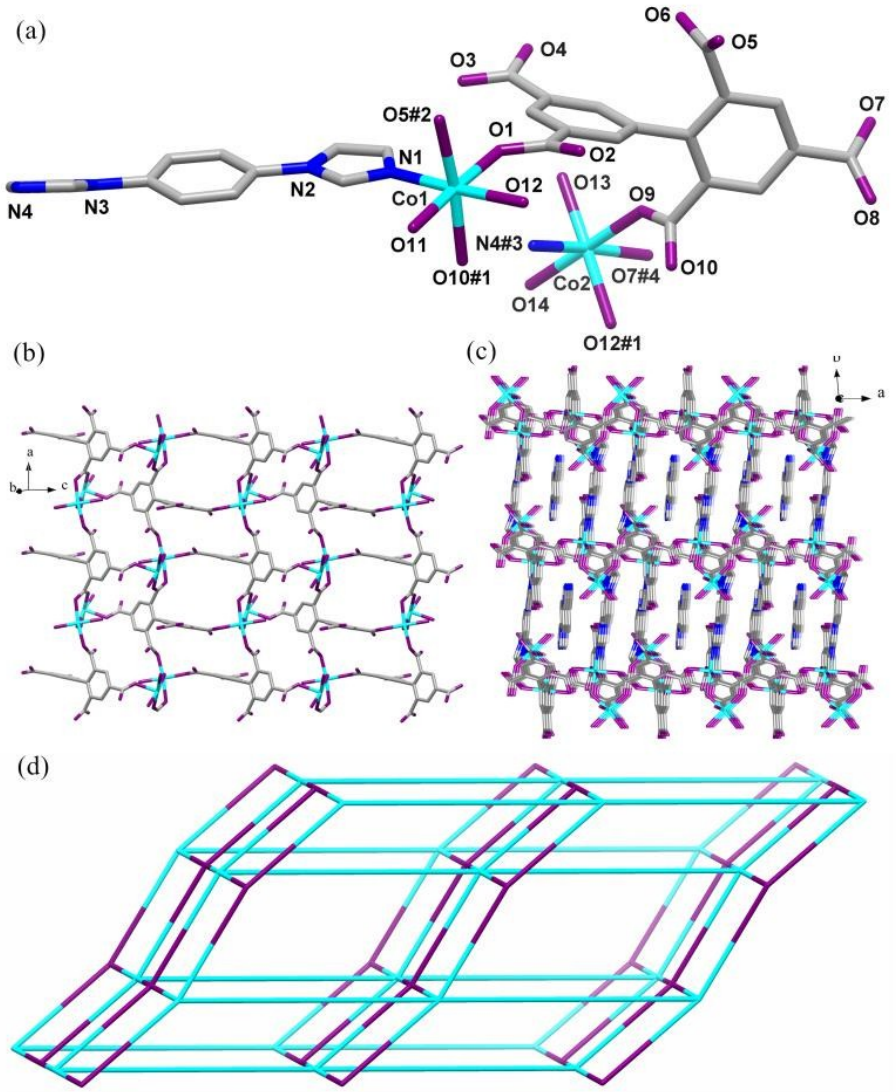

Fig. 5 (a) Coordination environments of Ni(II) ions in **5** (symmetry codes: #1, -x,-y+1,-z+1; #2, -x+1,-y+1,-z+1; #3, -x,-y,-z; #4, -x,-y+1,-z+2). (b) 2D layer constructed by Co(II) atoms and $bppc^{5-}$ligand. (c) View of the 3D architecture of **5**. (d) Schematic representation of the (4,6)-connected **fsc** net.

Synthetic Chemistry and Structural Diversity

Parallel experiments show that the pH values of the reaction system are crucial for formation of complexes **1**–**6**.[19] Complexes **1**–**6** could only be obtained in the special pH values. When the pH value is lower or higher than that special value, the expected crystals could not be obtained. When a molar ratio of 1:1:4:4 between $NaOH:H_5bppc:2,2'\text{-}bpy:Co^{2+}$ was used, a 0D structure, **1** was formed. In **1**, H_3bppc^{2-} is partly protonated and 2-carboxylate displays (κ^1,κ^1)-$\mu_2$coordination fashion to link two Co(II) atoms with Co···Co distance of 4.69 Å. 2,2'-bpy ligands act as terminal groups. And the ionized carboxyl groups interact with other binuclear units or free water, acting as hydrogen acceptor. So **1** has a 3D supramolecular architecture with $[Co_2(H_3bppc)_2(2,2'\text{-}bpy)_4]$ unit. When the amount of NaOH was increased to 2-fold of H_5bppc and added to the foregoing reaction systems, a 3D net **2** was obtained. In **2**, only one carboxylic group of multicarboxylic acid ligand is protonated and adopts the $(\kappa^1\text{-}\kappa^1)\text{-}(\kappa^1)\text{-}(\kappa^1)\text{-}(\kappa^1)\text{-}\mu_5$ coordination fashion to bridge five Co(II) atoms. The two adjacent Co1 are

Journal Name RSCPublishing

ARTICLE

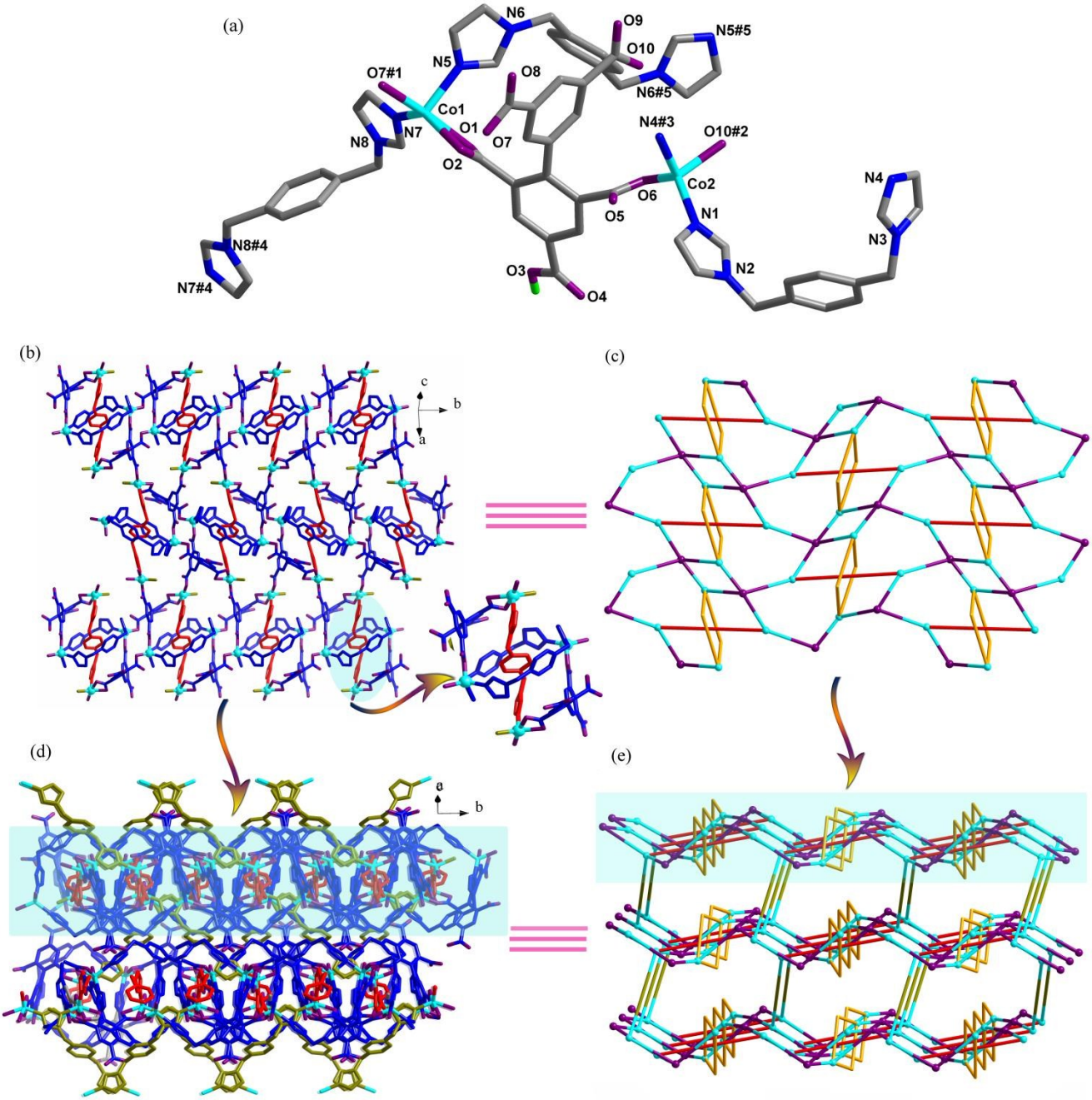

Fig. 6 (a) Coordination environments of Co(II) ions in **6** (symmetry codes: #1, -x+1,y-1/2,-z-1/2; #2, -x+2,-y+1,-z; #3, -x+2,-y+2,-z; #4, - x + 1, - y -1, - z; #5, - x +2, - y, - z). (b) View of 2D layer constructed by Co(II), $Hbppc^{4-}$, *cis*-bix, and *trans*-bix-A in **6**. (c) Schematic representation of the 2D layer. (d) View of the 3D architecture. (e) Schematic representation of the 3D net.

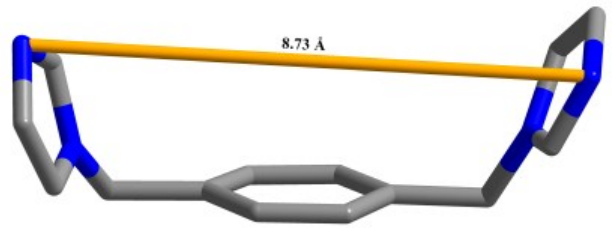

cix-bix

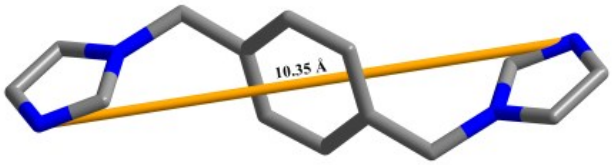

trans-bix-A

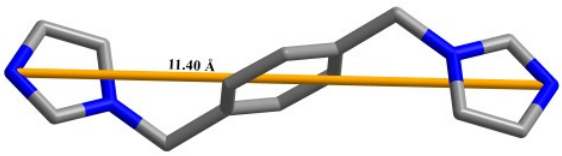

trans-bix-B

Scheme 3. Conformations of bix in **6**.

joined by two carboxylate groups of two $Hbppc^{4-}$ ligands to form a binuclear $[Co1_2(COO)_2(2,2'\text{-bpy})_4]^{2+}$ unit and 2,2'-bpy ligands act as terminal groups for Co1. The binuclear unit and Co2 atoms are linked by $Hbppc^{4-}$ ligands to generate a (3,4)-connected 3D **dmc** net. When a molar ratio of 2:1 between NaOH:H_5bppc was used for preparation of **2**–**6**, it is interesting to find out that the carboxylic groups of H_5bppc was partially deprotonated in **2**, **3** and **6** and fully deprotonated in **4** and **5**. When the amount of NaOH used for preparation of **2**, **3** and **6** was increased, by which we aim to obtain a product with complete deprotonation of all carboxylate groups. However, the results showed that only unknown deposit was obtained.

Since complexes **2**–**6** were assembled with the same carboxylic acid ligand, same metal salts, same solvent systems under the same temperature, the assembly process is tuned by different N-donor co-ligands. Complex **2** has been discussed above. So **3**–**6** are discussed here. In **3**, the bpp is partly protonated and acts as an unidentate ligand. The multicarboxylic acid ligand is partly protonated and shows (κ^1)-(κ^1)-(κ^1)-μ_3 coordination fashion. So **3** has a ladder-like array decorated with H-bpp. The protonated H-bpp and carboxyl groups interact with another 1D arrays, acting hydrogen bond acceptors. It is believed that the hydrogen bonds are critical in maintaining the overall 3D supramolecular structure. When dps is introduced, **4** is obtained. In **4**, $bppc^{5-}$ displays $(\kappa^1\text{-}\kappa^1)$-$(\kappa^1\text{-}\kappa^1)$-$(\kappa^1)$-$(\kappa^1\text{-}\kappa^1)$-$(\kappa^1\text{-}\kappa^1)$-$\mu_9$ binding fashion to link nine Co(II) atoms. Co1, Co2 and Co3 are bridged by the μ_3-hydroxyl group to form a trinuclear $[Co_3(\mu_3\text{-}OH)]^{5+}$ cluster. Such units are further linked by $bppc^{5-}$and dps ligands, giving rise to a binodal (5,7)-connected 3D network with a $(3.4^6.5^2.6)(3^2.4^6.5^7.6^5.7)$ topology.

When bib, a long bis(imidazole) ligand, is employed, **5** is obtained. In **5**, $bppc^{5-}$ ligand adopts the $(\kappa^1\text{-}\kappa^1)$-$(\kappa^1)$-$(\kappa^1)$-$(\kappa^1)$-$\mu_5$ coordination fashion to bridge five Co(II) atoms. Co1 and Co2#1 are linked by μ_2-H_2O and one carboxylic groups to form a binuclear $[Co_2(H_2O)(COO)]^{3+}$ unit. The binuclear units are bridged by $bppc^{5-}$ligands to form a 2D sheet and bib ligands act as pillars to join the 2D sheets into a 3D open network. Thus **5** has a (4,6)-connected 3D **fsc** net with binuclear $[Co_2(H_2O)(COO)]^{3+}$ units as nodes. The free volume of **5** is 20.9% of the crystal volume, and filled by H_2-bib and water molecules. When bix, a longer and more flexible ligand, is introduced, **6** shows a unique 3D network containing rare 2D polyrotaxane sheet. In **6**, $Hbppc^{4-}$ ligand links four Co(II) in the $(\kappa^1\text{-}\kappa^1)$-$(\kappa^1)$-$(\kappa^1)$-$(\kappa^1)$-$\mu_4$ coordination fashion. Co(II) atoms are joined by $Hbppc^{4-}$ and bix ligands to form a 3D net.

PXRD and TG Results

Complexes **1**–**6** are air stable, insoluble in common organic solvents, and can retain their crystalline integrity at ambient condition. In order to check the phase purity of complexes **1**–**6**, the powder X-ray diffraction (PXRD) patterns of these complexes were checked at room temperature. As shown in Fig. S3 (ESI), the peak positions of the simulated and experimental PXRD patterns are in agreement with each other, demonstrating the good phase purity of the complexes.

The thermal behaviors of **1**–**6** were studied by thermogravimetric analysis (TGA). The experiments were performed on samples consisting of numerous single crystals under air atmosphere with a heating rate of 10 °Cmin^{-1}, as shown in Fig. S4 (ESI). Complex **1** slowly lost a weight of 1.14% up to around 288 °C (calcd 1.19%) due to the loss of free water molecules, and then the framework began to decompose. For complex **2**, the first weight loss of 3.84% (calcd 4.30%) was observed from 30 to 160 °C corresponding to the loss of free and coordinated water molecules. The second process might start from 350 to 570 °C, indicating the decomposition of the coordination framework. The removal of free water molecules can be observed for **3** with the weight loss of 1.84% from 30 to 125 °C, corresponding to the loss of free water molecules (calcd 5.41%). The inconformity should be due to the loss of free water molecules in the air atmosphere. Then the curve reaches a plateau until 370 °C, the sharply weightlessness represents the structure collapse. For complex **4**, the weight loss of solvent molecules is observed at 15.26% (calcd 14.56%) in the temperature range of 55 to 165 °C. Then a sharp weight-loss step was observed between 355 to 450 °C. The TG curve of **5** shows a weight loss (9.90%) at 80-165 °C, corresponding to the loss of free water molecules and half of coordinated water molecules (calcd 9.68%). The removal of the organic components and other coordinated water molecules occurs in the range of 320-560 °C. For complex **6**, the free water molecules were lost from 55 to 90 °C (calcd 3.66%, found 3.14%) and the network was stable upon to 330 °C. Its mass remnant of 15.82% at ~560 °C corresponding to CoO (15.27% calcd).

Magnetic Properties

The magnetic susceptibilities, χ_M, of **1**–**6** were measured in the temperature range of 2-300 K at 1,000 Oe (Figs. 7 and 8). As the temperature was lowered to 2 K, the $\chi_M T$ value continuously decreased, which suggests that antiferromagnetic interactions are operative in **1**–**6**.

For complexes **1**, **2** and **5**, the experimental $\chi_M T$ value at room temperature is 5.46, 5.17 and 6.08 $cm^3 \cdot mol^{-1} \cdot K$, respectively, which is great larger than two isolated spin-only Co^{2+} cations

(3.75 $cm^3 \cdot mol^{-1} \cdot K$ with g = 2.0). The large value is due to the occurrence of an unquenched orbital contribution typical of the $^4T_{1g}$ ground state in six-coordinated Co(II) complexes.[20] The temperature dependence of the reciprocal susceptibilities ($1/\chi_M$) obeys the Curie-Weiss law above 5 K with a Weiss constant θ = -6.93 K, Curie constant C = 5.57 $cm^3 \cdot K \cdot mol^{-1}$ and R = 2.62 × 10^{-4} for **1**, θ = -7.64 K, C = 5.29 $cm^3 \cdot K \cdot mol^{-1}$ and R = 2.23 × 10^{-4} for **2** and θ = -16.64 K, C = 6.33 $cm^3 \cdot K \cdot mol^{-1}$ and R = 3.34 × 10^{-4} for **5** (the agreement factor $R = \sum[(\chi_M)_{obs} - (\chi_M)_{calc}]^2 / \sum[(\chi_M)_{obs}]^2$). The negative θ value also suggest that antiferromagnetic interactions are operative in **1**, **2** and **5**.

From the magnetic viewpoint, complexes **1** and **2** consists of binuclear Co(II) units bridged by two carboxylic groups in *syn-syn* fashion, which are further extended by hydrogen bonds or organic ligands linkers to give 3D structures. Thus, the magnetic susceptibility data were fitted assuming that the binuclear Co(II) units with exchange constant J. The susceptibility data were approximately analyzed by an isotropic dimer mode of spin S = 3/2.[21] The following eq 1 is induced from the Hamiltonian $\hat{H} = -J\hat{S}_1 \cdot \hat{S}_2$

$$\chi_M = \frac{Ng^2\beta^2}{KT}\frac{A}{B} \quad (1)$$

$$A = 2\exp[-2J/KT] + 10\exp[-6J/KT] + 28\exp[-12J/KT]$$

$$B = 1 + 3\exp[-2J/KT] + 5\exp[-6J/KT] + 7\exp[-12J/KT]$$

The least-squares analysis of magnetic susceptibilities data led to J = -1.70 cm^{-1}, g = 2.43 and R = 5.11 × 10^{-3} for **1**, J = -2.78 cm^{-1}, g = 2.38 and R = 1.39 × 10^{-4}above 50 K for **2**, and J = -2.99 cm^{-1}, g = 2.58 and R = 6.53 × 10^{-3} for **5**. The negative J value suggests that antiferromagnetic interactions between the adjacent Co(II) ions are mediated.

For complexes **3** and **6**, the experimental $\chi_M T$ value at 300 K is 3.26 and 2.80 $cm^3 \cdot mol^{-1} \cdot K$, which is larger than the spin-only value (1.875 $cm^3 \cdot mol^{-1} \cdot K$) expected for a magnetically isolated Co(II) ion. The magnetic susceptibilities data can be well fitted to the Curie-Weiss law with θ = -4.84 K, C = 3.21 $cm^3 \cdot K \cdot mol^{-1}$ and R = 8.10 × 10^{-4} for **3**, and θ = -1.84 K, C = 2.75 $cm^3 \cdot K \cdot mol^{-1}$ and R = 1.36 × 10^{-3} for **6**, revealing weak antiferromagnetic interactions between the adjacent Co(II) ions.

For complex **4**, the experimental $\chi_M T$ value at 300 K is 12.52 $cm^3 \cdot mol^{-1} \cdot K$, which is great larger than the spin-only value (5.625 $cm^3 \cdot mol^{-1} \cdot K$) expected for three magnetically isolated Co(II) ion. The magnetic susceptibilities data can be well fitted to the Curie-Weiss law above 50 K with θ = -86.99 K, C = 15.85 $cm^3 \cdot K \cdot mol^{-1}$ and R = 3.78 × 10^{-4} for **4**, revealing weak antiferromagnetic interactions between the adjacent Co(II) ions.

Among the superexchange pathways between the nearest neighboring Co^{II} ions, the large Co–O–Co angle and the *syn–syn* bridging mode of the carboxylate group are indication of antiferromagnetic interactions.[22] In **1** and **2**, the adjacent Co(II) atoms are linked by two μ_2-carboxylate groups in *syn-syn* fashion to form a $[Co_2(COO)_2(2,2'\text{-bpy})_4]$ unit. In **5**, the adjacent two Co(II) centre are linked by the one carboxylate groups and one μ_2-aqua to form a binuclear $[Co_2(H_2O)(COO)]^{3+}$ unit. The Co1–O12–Co2 angle is 122.17 °. So the antiferromagnetic interactions between Co^{II} ions would be expected. While in **4**, the antiferromagnetic interactions are found between Co^{II} ions in the trinuclear units relying on the effect of μ_3-hydroxyl group (Co–O–Co 118.24 °, 110.36 °) exchange pathway and *syn-syn* carboxylate exchange pathways.

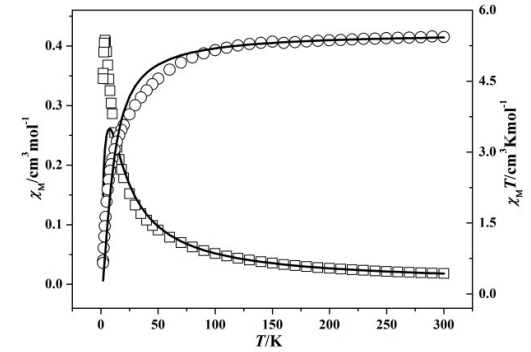

(**1**)

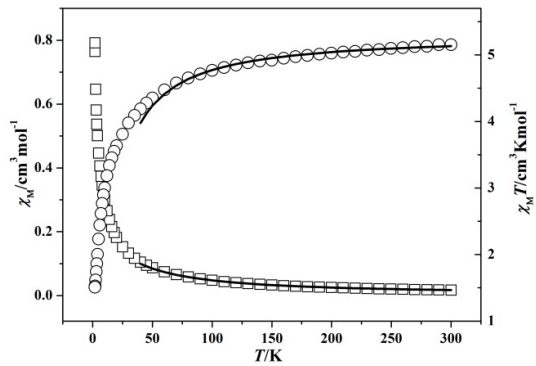

(**2**)

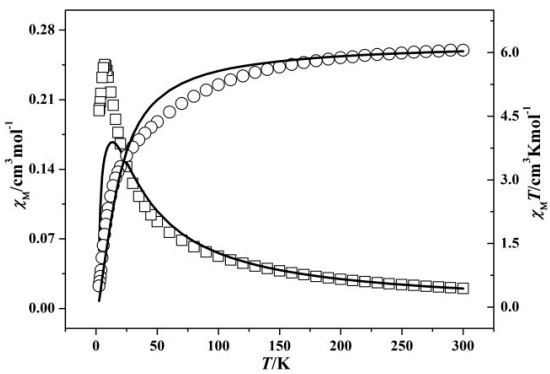

(**5**)

Fig. 7 Temperature dependence of $\chi_M T$ and χ_M versus T for **1**, **2** and **5**. Circle symbols represent $\chi_M T$ and square symbols represent χ_M. The solid lines represent the fits obtained from the Hamiltonian.

Conclusions

In short, six new Co(II) complexes, based on biphenyl-2,4,6,3',5'-pentacarboxylic acid, have been successfully synthesized and characterized. Complexes **1**–**6** display appealing structural features from 0D structure **1**, 1D ladder chains **3**, to 3D frameworks **2**, **4**–**6**. The topology studies reveal that the four 3D complexes possess different topologies: (3,4)-connected **dmc** net **2**, (5,7)-connected net **4**, (4,6)-connected **fsc** framework **5**, (3,4,4)-connected 3D network **6**, respectively. A detailed comparison of these complexes highlights that the pH value and N-donor co-ligands have an effect on the final structures. Magnetic studies of all six CPs indicate that all materials display weak antiferromagnetic behaviors. The results

demonstrate that pentacarboxylic acid may be used as a versatile building block to construct novel coordination polymers with fascinating structures and properties, also, further synthesis, structures and properties studies of other metal-coordination frameworks with the pentacarboxylic acid are under way in our lab.

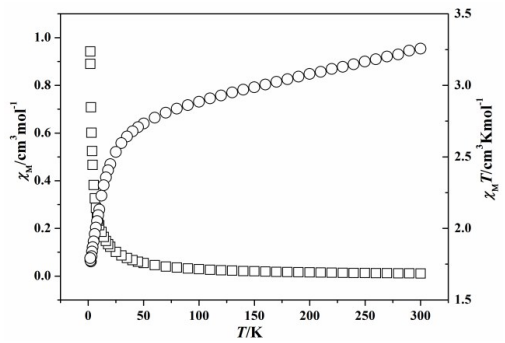

(**3**)

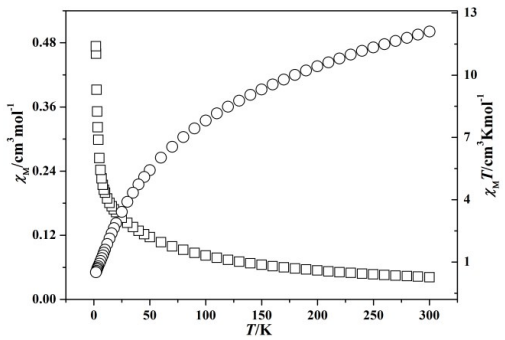

(**4**)

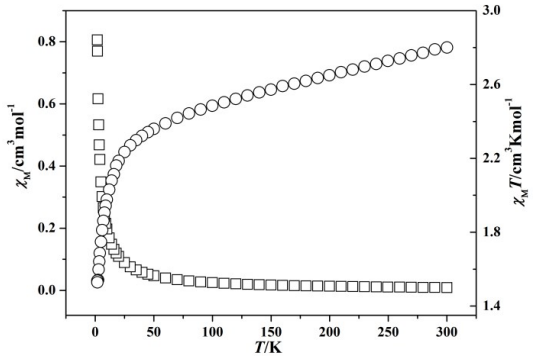

(**6**)

Fig. 8 Temperature dependence of $\chi_M T$ and χ_M versus T for **3**, **4** and **6**. Circle symbols represent $\chi_M T$ and square symbols represent χ_M.

Acknowledgements

This work was financially supported by NSF of China (Nos. 21201109 and 21373122) and NSF of Hubei Province of China (2011CDA118).

Notes and references

[a] Key Laboratory of Synthetic and Natural Functional Molecule Chemistry of the Ministry of Education, College of Chemistry & Materials Science, Northwest University, Xi'an 710069, P. R. China.

[b] College of Materials & Chemical Engineering, Collaborative Innovation Centre for Microgrid of New Energy of Hubei Province, China Three Gorges University, Yichang, 443002, China. Tel./Fax: +86-717-6397506; E-mail address: lidongsheng1@126.com (D.-S. Li).

Electronic Supplementary Information (ESI) available: X-ray crystallographic information for **1**–**6** in CIF format, Addition structure figure for **6**, PXRD patterns and TGA plots for **1**–**6**. See DOI: 10.1039/b000000x/

1 (*a*) J.-Y. Zhang, K. Wang, X.-B. Li, E.-Q. Gao, *Inorg. Chem.* 2014, **53**, 9306; (*b*) L.-Y. Du, H. Wang, G. Liu, D. Xie, F.-S. Guo, L. Hou, Y.-Y. Wang, *Dalton Trans.* 2015, **44**, 1110; (*c*) J. Palion-Gazda, T. Klemens, B. Machura, J. Vallejo, F. Lloret, M. Julve, *Dalton Trans.* 2015, **44**, 2989; (*d*) M. C. Bernini, J. R. de Paz, N. Snejko, R. Sáez-Puche, E. Gutierrez-Puebla, M. Á. Monge, *Inorg. Chem.* **2014**, **53**, 12885; (*e*) D.-S. Li, Y.-P. Wu, J. Zhao, J. Zhang, J. Y. Lu, *Coord. Chem. Rev.* 2014, **261**, 1; (*f*) K. Wang, H.-H. Zou, Z.-L. Chen, Z. Zhang, W.-Y. Sun, F.-P. Liang, *Dalton Trans.* 2014, **43**, 12989;

2 (*a*) R. Ding, C. Huang, J. Lu, J. Wang, C. Song, J. Wu, H. Hou, Y. Fan, *Inorg. Chem.* 2015, **54**, 1405; (*b*) H.-H. Li, Y.-J. Ma, Y. Q. Zhao, G.-H. Cui, *Transit. Metal Chem.* 2015, **40**, 21; (*c*) Y.-Q. Jiao, C. Qin, H.-Y. Zang, W.-C. Chen, C.-G. Wang, T.-T. Zheng, K.-Z. Shao, Z.-M. Su, *CrystEngComm* 2015, **17**, 2176; (*d*) J. Balapanuru, G. Chiu, C. Su, N. Zhou, Q.-H. Xu, K. P. Loh, *ACS Appl. Mater. Interfaces* 2015, **7**, 880; (*e*) S. Goberna-Ferrón, W. Y. Hernández, B. Rodríguez-García, J. R. Galán-Mascarós, *ACS Catal.* 2014, **4**, 1637.

3 (*a*) H.-R. Fu, Y. Kang, J. Zhang, *Inorg. Chem.* 2014, **53**, 4209; (*b*) M.-H. Zeng, Z. Yin, Y.-X. Tan, W.-X. Zhang, Y.-P. He, M. Kurmoo, *J. Am. Chem. Soc.* 2014, **136**, 4680; (*c*) S. K. Elsaidi, M. H. Mohamed, L. Wojtas, A. Chanthapally, T. Pham, B. Space, J. J. Vittal, M. J. Zaworotko, *J. Am. Chem. Soc.* 2014, **136**, 5072; (*d*) F. Yu, D.-D. Li, L. Cheng, Z. Yin, M.-H. Zeng, M. Kurmoo, *Inorg. Chem.* 2015, **54**, 1655; (*e*) K. Su, F. Jiang, J. Qian, J. Pang, F. Hu, S. M. Bawaked, M. Mokhtar, S. A. Al-Thabaiti, M. Hong, *CrystEngComm* 2015, **17**, 1750; (*f*) M. Chen, H. Zhao, C.-S. Liu, X. Wang, H.-Z. Shi and M. Du, *Chem. Commun.* 2015, **51**, 6014.

4 (*a*) N. Zhao, Y.-E. Deng, P. Liu, C.-X. An, T.-X. Wang, Z.-X. Lian, *Transit. Metal Chem.* 2015, **40**, 11; (*b*) N. Zhao, P. Liu, C.-X. An, T.-X. Wang, Z.-X. Lian, *Inorg. Chem. Commun.* 2014, **50**, 97; (*c*) S. Mendiratta, M. Usman, T.-T. Luo, B.-C. Chang, S.-F. Lee, Y.-C. Lin, K.-L. Lu, *Cryst. Growth Des.* 2014, **14**, 1572; (*d*) L. Wen, L. Zhou, B. Zhang, X. Meng, H. Qu, D. Li, *J. Mater. Chem.* 2012, **22**, 22603.

5 (*a*) H.-S. Lu, L. Bai, W.-W. Xiong, P. Li, J. Ding, G. Zhang, T. Wu, Y. Zhao, J.-M. Lee, Y. Yang, B. Geng, Q. Zhang, *Inorg. Chem.* 2014, **53**, 8529; (*b*) J. Wang, X. Jing, Y. Cao, G. Li, Q. Huo, Y. Liu, *CrystEngComm* 2015, **17**, 604; (*c*) L. Xu, B. Liu, S.-X. Liu, H. Jiao, B. de Castro, L. Cunha-Silva, *CrystEngComm* **2014**, *16*, 10649; (*d*) M. T. Kapelewski, S. J. Geier, M. R. Hudson, D. Stück, J. A. Mason, J. N. Nelson, D. J. Xiao, Z. Hulvey, E. Gilmour, S. A. FitzGerald, M. Head-Gordon, C. M. Brown, J. R. Long, *J. Am. Chem. Soc.* 2014, **136**, 12119; (*e*) Z. Zhu, Y.-L. Bai, L. Zhang, D. Sun, J. Fang, S. Zhu, *Chem. Commun.* 2014, **50**, 14674; (*f*) J. Wang, J. Luo, J. Zhao, D.-S. Li, G. Li, Q. Huo, Y. Liu, *Cryst. Growth Des.* 2014, **14**, 2375; (*g*) J. Li, J. Tao, R.-B. Huang, L.-S. Zheng, *Inorg. Chem.* 2012, **51**, 5988.

6 (*a*) Z. Zhang, M. J. Zaworotko, *Chem. Soc. Rev.* 2014, **43**, 5444; (*b*) W. Lu, Z. Wei, Z.-Y. Gu, T.-F. Liu, J. Park, J. Park, J. Tian, M. Zhang, Q. Zhang, T. Gentle III, M. Bosch, H.-C. Zhou, *Chem. Soc. Rev.* 2014, **43**, 5561; (*c*) Z.-J. Lin, J. Lü, M. Hong, R. Cao, *Chem. Soc. Rev*. 2014, **43**, 5867; (*d*) V. Guillerm, D. Kim, J. F. Eubank, R. Luebke, X. Liu, K. Adil, M. S. Lah, M. Eddaoudi, *Chem. Soc. Rev.* 2014, **43**, 6141; (*e*) M. Du, C.-P. Li, C.-S. Liu, S.-M. Fang, *Coord. Chem. Rev*. 2013, **257**, 1282; (*f*) M. P. Suh, H. J. Park, T. K. Prasad, D.-W. Lim, *Chem. Rev*. 2012, **112**, 782.

7 (*a*) L.-X. You, S.-J. Wang, G. Xiong, F. Ding, K. W. Meert, D. Poelman, P. F. Smet, B.-Y. Ren, Y.-W. Tian, Y.-G. Sun, *Dalton Trans.* 2014, **43**, 17385; (*b*) L. Hou, B. Liu, L.-N. Jia, L. Wei, Y.-Y. Wang, Q.-Z. Shi, *Cryst. Growth Des.* 2013, **13**, 701; (*c*) C.-L. Zhang, L. Qin, Z.-Z. Shi, H.-G. Zheng, *Dalton Trans*. 2015, **44**, 4238.

8 L. Bai, H.-B. Wang, D.-S. Li, Y.-P. Wu, J. Zhao, L.-F. Ma, *Inorg. Chem. Commun.* 2014, **44**, 188.

9 (*a*) J.-Q. Liu, J. Wu, Y.-Y. Wang, J.-T. Liu, H. Sakiyama, *CrystEngComm* 2014, **16**, 3103; (*b*) C. Tian, Z. Lin, S. Du, *Cryst. Growth Des*. 2013, **13**, 3746; (*c*) S.-Q. Zang, M.-M. Dong, Y.-J. Fan, H.-W. Hou, T. C. W. Mak, *Cryst. Growth Des.* 2012, **12**, 1239; (*d*) X.-H. Chang, L.-F. Ma, H. Guo, L.-Y. Wang, *Cryst. Growth Des.* 2012, **12**, 3638; (*e*) Y. Bu, F. Jiang, K. Zhou, Y. Gai, M. Hong, *CrystEngComm* 2014, **16**, 1249; (*f*) Z.-X. Xu, Y.-X. Tan, H.-R. Fu, Y. Kang, J. Zhang, *Chem. Commun*. 2015, **51**, 2565.

10 (*a*) X. Zhu, P.-P. Sun, J.-G. Ding, B.-L. Li, H.-Y. Li, *Cryst. Growth Des.* 2009, **9**, 3992; (*b*) B. Li, X. Zhou, Q. Zhou, G. Li, J. Hua, Y. Bi, Y. Li, Z. Shi, S. Feng, *CrystEngComm* 2011, **13**, 4592; (*c*) Y. Fu, J. Su, S. Yang, G. Li, F. Liao, M. Xiong, J. Lin, *Inorg. Chim. Acta* 2010, **363**, 645; (*d*) F. Wang, H.-R. Fu, Y. Kang, J. Zhang, *Chem. Commun*. 2015, **51**, 12065; (*e*) F. Luo, Y. Ning, X.-L. Tong, M.-B. Luo, *Inorg. Chem. Commun*.2010, **13**, 671; (*f*) H.-R. Fu, J. Zhang, *Chem.-Eur. J*. 2015, **21**, 5700.

11 (*a*) X.-X. Lu, Y.-H. Luo, Y. Xu, H. Zhang, *CrystEngComm* 2015, **17**, 1631; (*b*) M.-L. Han, Y. Zhao, D.-S. Li, Y.-P. Wu, L.-F. Ma, *Inorg. Chem. Commun*. 2015, **52**, 1; (*c*) L. Fan, W. Fan, B. Li, X. Liu, X. Zhao, X. Zhang, *Dalton Trans*. 2015, **44**, 2380; (*d*) T.-T. Wu, W. Hsu, X.-K. Yang, H.-Y. He, J.-D. Chen, *CrystEngComm* 2015, **17**, 916; (*e*) X.-L. Chi, J.-L. Liu, H.-Y. Chen, J. Yang, H.-Y. Zhang, J.-L. Zhang, Y. Chen, Q. Yang, D.-R. Xiao, *Inorg. Chem. Commun.* 2014, **50**, 101; (*f*) S.-Y. Ke, Y.-F. Chang, H.-Y. Wang, C.-C. Yang, C.-W. Ni, G.-Y. Lin, T.-T. Chen, M.-L. Ho, G.-H. Lee, Y.-C. Chuang, C.-C. Wang, *Cryst. Growth Des*. 2014, **14**, 4011.

12 (*a*) I.-H. Park, R. Medishetty, J.-Y. Kim, S. S. Lee, J. J. Vittal, *Angew. Chem. Int. Ed.* 2014, **53**, 5591; (*b*) J.-X. Yang, Y.-Y. Qin, J.-K. Cheng, Y.-G. Yao, *Cryst. Growth Des.* 2014, **14**, 1047; (*c*) X. Zhang, L. Fan, W. Zhang, W. Fan, L. Sun, X. Zhao, *CrystEngComm* 2014, **16**, 3203; (*d*) H. Wu, X.-L. Lu, C.-L. Yang, C.-X. Dong, M.-S. Wu, *CrystEngComm* 2014, **16**, 992; (*e*) M. Li, S. Zhao, Y.-F. Peng, B.-L. Li, H.-Y. Li, *Dalton Trans*. 2013, **42**, 9771; (f) J. Wu, J.-Q. Liu, J.-T. Lin, T. Wu, X.-R. Wu, C.-H. Zhou, X.-Y. Qin, *Inorg. Chim. Acta* 2013, **405**, 65.

13 (*a*) T. Cao, Y. Peng, T. Liu, S. Wang, J. Dou, Y. Li, Y. Zhou, D. Li, J. Bai, *CrystEngComm* 2014, **16**, 10658; (*b*) H. C. Garcia, R. Diniz, L. F. C. de Oliveira, *Polyhedron* 2013, **53**, 40; (*c*) M.-L. Han, S.-H. Li, L.-F. Ma, L.-Y. Wang, *Inorg. Chem. Commun.* 2012, **20**, 340; (*d*) H.-W. Kuai, T. Okamura, W.-Y. Sun, *Polyhedron* 2014, **72**, 8; (*e*) S. Wöhlert, L. Fink, M. U. Schmidt, C. Näther, *Z. Anorg. Allg. Chem.* 2013, **639**, 2186; (*f*) L.-F. Ma, L.-Y. Wang, Y.-Y. Wang, M. Du, J.-G. Wang, *CrystEngComm* 2009, **11**, 109.

14 (*a*) D.-S. Li, J. Zhao, Y.-P. Wu, B. Liu, L. Bai, K. Zou, M. Du, *Inorg. Chem.* 2013, **52**, 8091; (*b*) J. Zhao, W.-W. Dong, Y.-P. Wu, Y.-N. Wang, C. Wang, D.-S. Li, Q.-C. Zhang, *J. Mater. Chem. A* 2015, **3**, 6962; (*c*) M.-L. Han, Y.-P. Duan, D.-S. Li, G.-W. Xu, Y.-P. Wu, J. Zhao, *Dalton Trans*. 2014, **43**, 17519; (*d*) M.-L. Han, Y.-P. Duan, D.-S. Li, H.-B. Wang, J. Zhao, Y.-Y. Wang, *Dalton Trans*. 2014, **43**, 15450; (*e*) B. Liu, J. Shi, K.-F. Yue, D.-S. Li, Y.-Y. Wang, *Cryst. Growth Des.*2014, **14**, 2003; (*f*) W.-W. Dong, D.-S. Li, J. Zhao, Y.-P. Duan, L. Bai, J.-J. Yang, *RSC Adv*. 2012, **2**, 11219; (*g*) J. Zhao, D.-S. Li, X.-J. Ke, B. Liu, K. Zou, H.-M. Hu, *Dalton Trans*. 2012, **41**, 2560; (*h*) D.-S. Li, F. Fu, J. Zhao, Y.-P. Wu, M. Du, K. Zou, W.-W. Dong, Y.-Y. Wang, *Dalton Trans*. 2010, **39**, 11522; (*i*) F. Fu, D.-S. Li, Y.-P. Wu, X.-M. Gao, M. Du, L. Tang, X.-N. Zhang, C.-X. Meng, *CrystEngComm* 2010, **12**, 1227; (*j*) G.-W. Xu, Z.-L. Wang, G.-X. Wen, S.-S. Guo, D.-S. Li, J. Zhang, *Inorg. Chem. Commun.* 2015, **55**, 17; (*k*) Y.-Q. Mu, B.-F. Zhu, D.-S. Li, D. Guo, J. Zhao, L.-F. Ma, *Inorg. Chem. Commun*. 2013, **33**, 86.

15 A. L. Spek, *J. Appl. Crystallogr*.2003, **36**, 7.

16 (*a*) L. Fan, Y. Gao, G. Liu, W. Fan, W. Song, L. Sun, X. Zhao, X. Zhang, *CrystEngComm* 2014, **16**, 7649; (*b*) G.-X. Liu, K. Zhu, H.-M. Xu, S. Nishihara, R.-Y. Huang, X.-M. Ren, *CrystEngComm* 2010, **12**, 1175.

17 J. Yang, J.-F. Ma, S. R. Batten, Z.-M. Su, *Chem. Commun.* **2008**, 2233.

18 (*a*) L.-F. Ma, Q.-L. Meng, C.-P. Li, B. Li,; Wang, L.-Y.; Du, M.; Liang, F.-P. *Cryst. Growth Des.* 2010, **10**, 3036; (*b*) M.-D. Zhang, C.-M. Di, L. Qin, Q.-X. Yang, Y.-Z. Li, Z.-J. Guo, H.-G. Zheng, *CrystEngComm* 2013, **15**, 227; (*c*) I.-H. Park, R. Medishetty, S. S. Lee, J. J. Vittal, *Chem. Commun.* 2014, **50**, 6585.

19 (*a*) S.-M. Fang, Q. Zhang, M. Hu, E. C. Sañudo, M. Du, C.-S. Liu, *Inorg. Chem.* 2010, **49**, 9617; (*b*) C-P. Li, Q. Yu, J. Chen, M. Du, *Cryst. Growth Des.* 2010, **10**, 2650.

20 (*a*) R. L. Carlin, *Magnetochemistry*; Springer-Verlag: Berlin, Heidelberg, **1986**. (*b*) F. E. Mabbs, D. J. Machin, *Magnetism and Transition Metal Complexes*; Chapman and Hall Ltd.: London, **1973**.

21 C. J. O'Connor, *Prog. Inorg. Chem.* 1982, **29**, 203-283.

22 (*a*) L.-F. Ma, Y.-Y. Wang, L.-Y. Wang, D.-H. Lu, S. R. Batten, J.-G. Wang, *Cryst. Groth Des.* 2009, **9**, 2036; (*b*) Q. Chen, J.-B. Lin, W. Xue, M.-H. Zeng, X.-M. Chen, *Inorg. Chem.* 2011, **50**, 2321; (*c*) P. Alborés, E. Rentschler, *Dalton Trans.* **2009**, 2609; (*d*) J. Cui, Y. Li, Z. Guo, H. Zheng, *Cryst. Growth Des.* 2012, **12**, 3610.

